the plant journal

SEB SOCIETY FOR EXPERIMENTAL BIOLOGY

The Plant Journal (2025) **123,** e70456 doi: 10.1111/tpj.70456

Tandem gene duplication facilitates intertidal adaptation in atypical mangrove plants

Yulong Li, Shao Shao, Ranran Zhu, Yarong Wang, Chuanfeng Jin, Min Liu, Kaichi Huang, Zixiao Guo, Ziwen He, Suhua Shi* and Shaohua Xu*

State Key Laboratory of Biocontrol and Guangdong Provincial Key Laboratory of Plant Stress Biology, Innovation Center for Evolutionary Synthetic Biology, School of Ecology and School of Life Sciences, Sun Yat-sen University, Guangdong, China

Received 18 March 2025; revised 28 July 2025; accepted 18 August 2025.
*For correspondence (e-mail lssssh@mail.sysu.edu.cn and xushh27@mail.sysu.edu.cn).

SUMMARY

Mangrove plants, originating from inland ancestors, have independently adapted to extreme intertidal zones characterized by salt and hypoxia stress. While typical mangroves exhibit specialized phenotypes, like viviparous seeds and salt secretion, atypical clades that have thrived without such traits are particularly suitable for exploring the molecular and physiological basis underlying plant adaptation to intertidal zones. We assembled a chromosome-level genome of an atypical mangrove, *Scyphiphora hydrophylacea*, the only mangrove species in Gentianales. Similar to other mangroves, *S. hydrophylacea* colonized intertidal zones during climatic optimum periods of sea-level rise. Despite lacking recent whole-genome duplications (WGDs), its genome acquired extensive tandem gene duplications (TDs), leading to the rapid expansion of key salt- and hypoxia-related genes. Transcriptome data further corroborated that TD-driven gene expansions contribute to stress tolerance. Specifically, the expansion of genes involved in cation transmembrane transport, osmotic regulation, and oxidative stress response may enhance salinity tolerance, and the expansion of signal transduction and energy metabolism genes in hypoxia-response pathways may confer waterlogging tolerance. Therefore, in the absence of large-scale gene duplication, the rapid expansion of core genes involved in salt and hypoxia tolerance through tandem duplication may represent a key force driving the adaptation of atypical mangroves. These findings also provide valuable insights for crop improvement strategies aimed at enhancing environmental resilience while maintaining phenotypic stability.

Keywords: *Scyphiphora hydrophylacea*, atypical mangrove, genome evolution, tandem gene duplication, salt tolerance, hypoxia tolerance.

INTRODUCTION

Identifying key genetic changes responsible for plant stress adaptation is crucial for understanding how plants cope with their environments. However, adaptations that occurred millions of years ago are often difficult to trace, as they are masked by extensive genetic changes unrelated to environmental pressures. Additionally, plants usually exhibit diverse adaptations to the same environmental stresses. Despite this diversity in phenotypic and genetic responses, identifying fundamental molecular mechanisms driving these adaptations is essential for evolutionary biology and practical applications.

Mangrove plants exemplify this challenge, as they have independently colonized stressful intertidal zones while evolving diverse strategies to cope with high salinity and waterlogging (He et al., 2022). Most previous research has focused on typical mangroves exhibiting phenotypic traits such as viviparous seeds, salt secretion, aerial roots, and high tannin content (Ball, 1988; Mimura et al., 2003; Parida & Jha, 2010; Sudhir et al., 2022; Tomlinson, 2016) (Figure 1). Although these phenotypic traits play crucial roles in environmental adaptation, they are usually distributed in only a subset of mangrove clades (Tomlinson, 2016). For example, viviparous seeds have evolved in only six (Rhizophoreae, *Avicennia*, *Aegiceras*, *Aegialitis*, *Pelliciera*, and *Nypa*) of over 20 mangrove clades, while salt glands are present in only five (Elmqvist & Cox, 1996; Shi et al., 2005; Srikanth et al., 2016; Tomlinson, 2016). Despite the possible large selective advantage, the evolution of phenotypic traits is usually complex and involves the long-term evolution of a large number of genes (Hagolani et al., 2021; Medina-Gomez et al., 2017; Plata et al., 2015). The variety and difficulty in evolution suggest that adaptive phenotypes may not be the fundamental

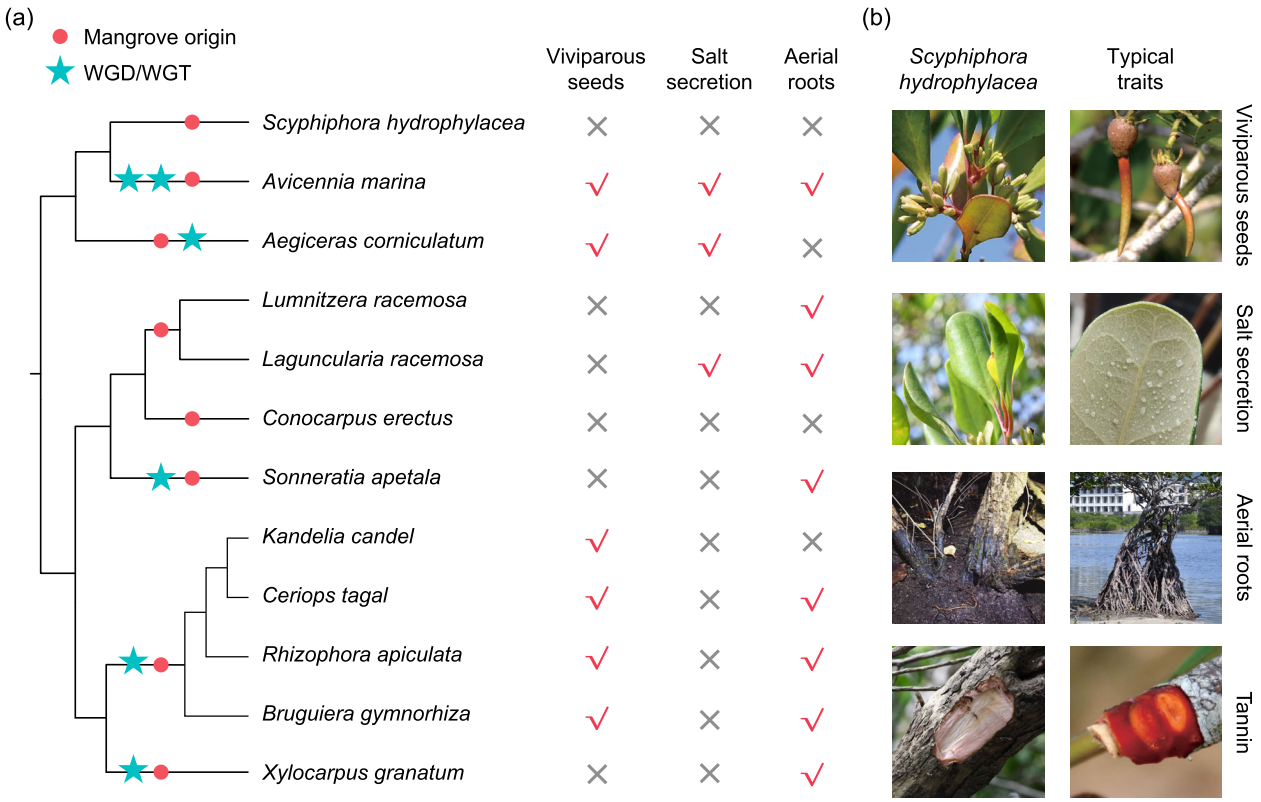

Figure 1. Typical phenotypic traits of representative mangrove clades.
(a) Presence or absence of specialized phenotypic traits across eight mangrove clades. Red dots on the phylogenetic tree indicate independent origins of mangrove lineages. Whole-genome duplication and triplication (WGD and WGT) events identified in previous studies are marked with stars.
(b) Comparison of phenotypic characteristics between *Scyphiphora hydrophylacea* and typical mangrove traits.

molecular mechanisms essential for intertidal environment adaptation.

Meanwhile, many mangrove species, such as *Scyphiphora hydrophylacea* and *Conocarpus erectus*, lack such specialized traits yet still thrive in intertidal environments (Duke, 2013; Tomlinson, 2016). Without the evolution of complex phenotypic traits, these "atypical" mangroves are likely to have targetedly modified stress-response pathways at molecular and physiological levels. It makes them excellent models for exploring the fundamental adaptation mechanisms of intertidal environments, especially the high salinity and waterlogging. Despite their ecological significance, genomic studies on atypical mangroves remain scarce, limiting our understanding of how they achieve such adaptations without typical morphological traits. Expanding genomic investigations into these species will be crucial for identifying fundamental mechanisms underlying intertidal adaptation and complementing existing knowledge derived primarily from typical mangroves.

We also noticed that many typical mangrove clades have experienced whole-genome duplications (WGDs), which duplicate the entire genomic DNA and provide abundant material for environmental adaptation and trait innovation in plants (Almeida-Silva & Van de Peer, 2023; Wu et al., 2020). Previous studies have found that the WGD events of typical mangroves contributed to functional divergence, genetic redundancy, and evolution of novel traits (Figure 1) (Adams & Wendel, 2005; Conant & Wolfe, 2008; Feng et al., 2021; Feng et al., 2024; Wu et al., 2020; Xu et al., 2017; Xu et al., 2021). But there are also mangrove clades without WGDs, such as the mangroves in Combretaceae (Xie et al., 2023; Zhu et al., 2023). The molecular mechanisms underlying the environmental tolerance of these atypical mangroves remain poorly understood. Tandem gene duplications (TDs) play a significant role in adaptive responses to environmental stimuli by rapidly and selectively expanding crucial genes, thereby enabling fine-tuned adjustments to the genetic makeup (Hanada et al., 2008). For instance, in salt cress and desert poplar, TDs of *HKT1* and *NHX* are thought to enhance salinity tolerance (Ma et al., 2013; Oh et al., 2014; Wu et al., 2012). Similarly, TD-mediated expansion of stress-responsive genes may provide a fundamental genetic basis for the adaptation of atypical mangroves to intertidal environments.

Scyphiphora hydrophylacea C. F. Gaertner is an atypical mangrove species widely distributed across the Indo-West Pacific (IWP) region (Duke, 2013). Despite lacking above specialized traits, *S. hydrophylacea* exhibits high salt and hypoxia tolerance (Giesen et al., 2007; Guo et al., 2018; Wang et al., 2011). Based on our field investigation, *S. hydrophylacea* individuals are capable of withstanding tidal inundation with seawater salinity of 30‰ for up to 6 h during high tide cycles (Figure S1). As a non-secretor species, it copes with excess salt by transporting it into leaf vacuoles, which are later shed as the leaves senesce (Wang et al., 2011). Notably, *S. hydrophylacea* is the only mangrove species within the order Gentianales, which contains over 23,000 species (https://wfoplantlist.org/). As the sole mangrove representative of such a diverse clade, it is likely in the early stage of tidal zone colonization, making it an ideal model for studying the molecular basis of intertidal environmental adaptation.

In this study, we assembled a high-quality reference genome for the atypical mangrove *Scyphiphora hydrophylacea*. Using comparative genomics and transcriptome analyses, we investigated the molecular mechanisms underlying its adaptation to the primary stressors of intertidal zones. Our findings suggest that extensive tandem gene duplications play a key role in facilitating the adaptation of atypical mangroves to intertidal habitats by duplicating essential genes involved in salt and hypoxia tolerance. These results highlight the importance of TDs as a significant genetic mechanism driving adaptation to extreme intertidal environments.

RESULTS

A high-quality genome assembly of *S. hydrophylacea*

To conduct genome assembly of *Scyphiphora hydrophylacea*, we obtained approximately 161.9 Gb of 10× Genomics linked reads (~140-fold coverage), 34.8 Gb of paired-end short reads (~40-fold coverage), and 153.9 Gb of Hi-C reads (~160-fold coverage) (Table S1). The assembly was 1234 Mb, covering 90.6% of the estimated genome size, with a scaffold N50 length of 99.2 Mb (Table 1; Table S3; Figure S2). We could anchor 1129.5 Mb (91.5%) of the genome assembly onto 11 pseudo-chromosomes, ranging from 80.5 to 144.5 Mb (Table S2; Figure 2a; Figure S4a). In this assembly, 99.4% of short reads were adequately mapped, and 96.3% of BUSCO eudicot markers were detected with complete structure (Table 1; Figure S3). These results indicate a high level of completeness and accuracy in the *S. hydrophylacea* genome assembly.

Using a combination of database-based annotation and *de novo* prediction, we identified 65.0% (816 Mb) of repetitive sequences on the genome assembly (Table S4). After masking the repetitive sequences, we predicted a total of 30,380 protein-coding genes, representing 7.5% (92.2 Mb) of the genome assembly. Among these predicted genes, 27,348 (90.0%) were located on the 11 pseudo-chromosomes, and 29,109 (95.8%) were functionally annotated using a combination of NR, Swiss-Prot, KEGG, KOG, TrEMBL, InterPro, and GO databases (Figures S4 and S5).

Table 1 Summary statistics of *Scyphiphora hydrophylacea* genome assembly and annotation

Statistics	Assessment
Assembly feature	
Estimated genome size	1362 Mb
Assembled genome size	1234 Mb
No. of chromosomes	11
N50 length	99.2 Mb
L50 count	6
GC content	33.7%
Completeness assessment	
Complete BUSCOs	96.3%
Raw reads mapping rate	99.4%
Genome annotation	
Protein-coding genes	30380
Repetitive sequence	65.0% (816 Mb)

S. hydrophylacea originated during global warming

By clustering homologous genes across species, a total of 1262 single-copy orthologous genes were obtained for phylogeny reconstruction and divergence time estimation. The stem age and crown age of Gentianales were estimated to be 79.5 million years ago (Mya) and 60.4 Mya, respectively. *S. hydrophylacea* was found to diverge with *Coffea canephora* at approximately 18.1 Mya. Considering that *Scyphiphora* fossils have been reported at the Miocene—around 16 Mya from Japan (Tsuda et al., 1984), the differentiation time was finally determined to be between 18.1 and 16 Mya (Figure 2b). This period corresponds to the mid-Miocene climatic optimum (MMCO), which occurred between 17 and 15 Mya (Zachos et al., 2001). The MMCO was characterized by reduced ice volumes, a significantly warmer global mean annual temperature of 18–18.4°C, and a notable rise in global sea level of up to ~50 m compared with the previous period (Goldner et al., 2014; Miller et al., 2020; Reuter et al., 2021; You et al., 2009). The rising sea levels may have facilitated the transition of land-based species into coastal habitats.

Lack of recent whole-genome duplication (WGD) event in *S. hydrophylacea*

Utilizing gene family clustering, we categorized the protein-coding genes in *S. hydrophylacea* into 18,887 orthogroups, of which 8145 were shared across all nine species. Gene family evolution analysis, based on the phylogenetic tree and gene family clusters, identified 318

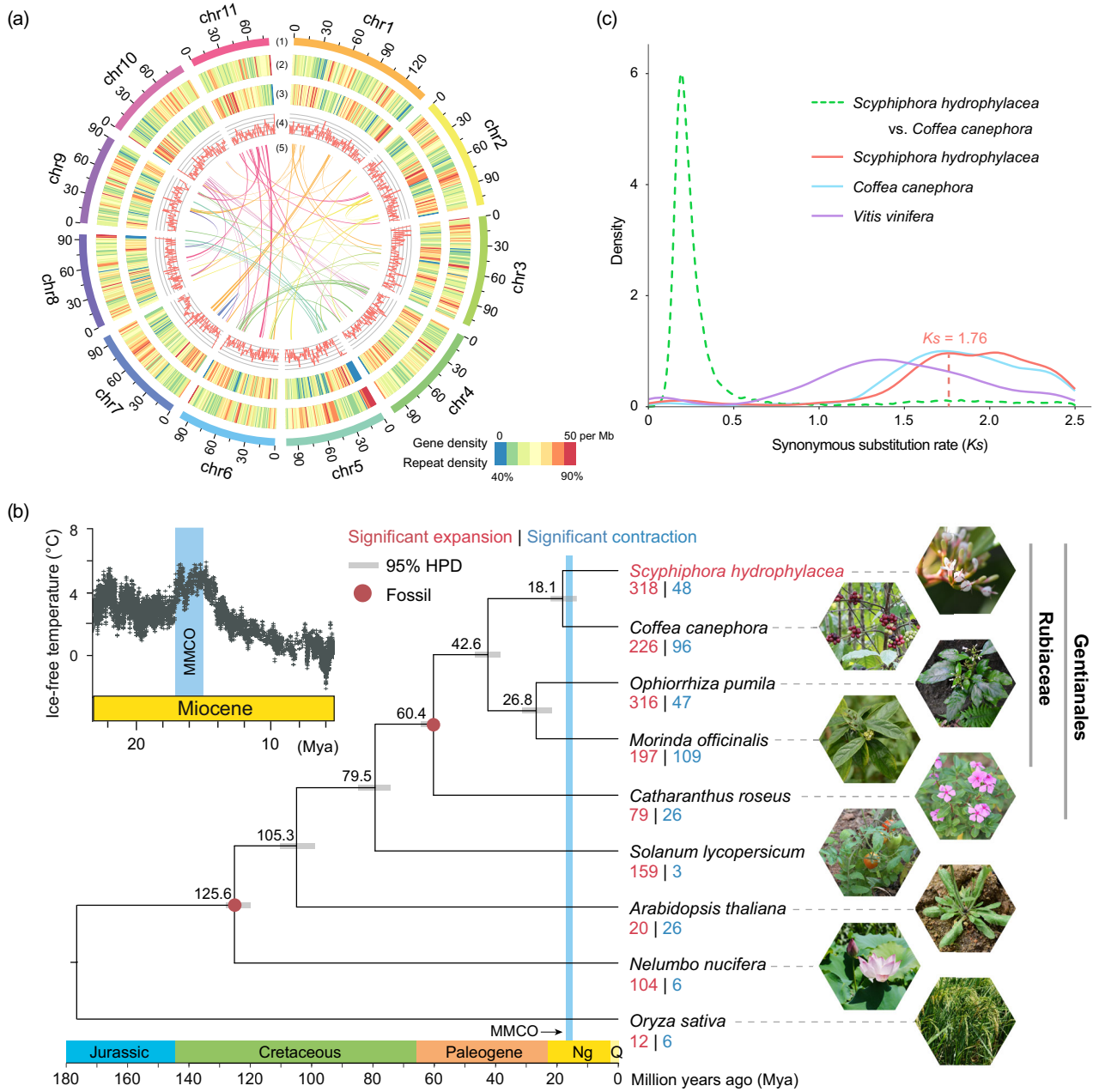

Figure 2. Genome feature and phylogeny of *Scyphiphora hydrophylacea*.
(a) Circos diagram of the genome assembly (window size = 1 Mb, 0.1% of genome size). From outer to inner rings: (1) Chromosomal structure; (2) Repetitive sequence density (42.57–92.89%, mean: 64.57% ± 9.00%); (3) Gene density (24 ± 10 genes per Mb); (4) GC content (27.04–39.90%, mean: 31.56% ± 1.42%); (5) Collinearity within *S. hydrophylacea*. Each line represents a collinear gene pair, and each cluster of lines corresponds to a collinear block.
(b) Divergence time estimation and gene family expansion/contraction in *S. hydrophylacea* and related species. Gray bars represent the 95% highest posterior density (HPD) intervals, and the red dots indicate fossil calibration points. Numbers below species names represent rapidly expanded and contracted gene families. MMCO is the abbreviation for the mid-Miocene climatic optimum. The photo of *Ophiorrhiza pumila* is sourced from iNaturalist (https://www.inaturalist.org/) and credited to Chiqian Fan. The photos of *Morinda officinalis* and *Arabidopsis thaliana* are from the Plant Photo Bank of China (PPBC, https://ppbc.iplant.cn/) and credited to Youpai Zeng and Xinxin Zhu, respectively. The inset on the top left showing historical climate change is adapted from Zachos et al., 2008.
(c) Distribution of synonymous substitution rates (*Ks*) among collinear genes within and between species. The absence of a recent *Ks* peak for *S. hydrophylacea* suggests no recent WGD event.

significantly expanded and 48 significantly contracted gene families (Figure 2b). The expanded gene families were significantly enriched in functions related to cation transmembrane transport, calcium transport and signaling, S-glycoside metabolism, and brassinosteroid metabolism (*P-adj* <0.05; Figures S6 and S7).

We first investigated whether the gene expansions were produced by WGDs. We totally identified 1067 collinear gene pairs (including 1994 genes, 6.6% of the total genes) distributed across 103 collinear blocks in the *S. hydrophylacea* genome (Figure 2a). The relatively low number of collinear gene pairs suggests that this lineage may not have undergone a substantial recent WGD event. The distribution of synonymous substitution per synonymous site (*Ks*) for these collinear homologous genes showed a peak at 1.76, corresponding to the well-known paleo-hexaploidization event (γ event) at the last common ancestor of eudicots (Figure 2c). Similarly, none of the other four Gentianales species (*Coffea canephora*, *Morinda officinalis*, *Catharanthus roseus* and *Ophiorrhiza pumila*) exhibited recent *Ks* peaks. We further confirmed these findings by identifying a 1:1 collinear relationship between *S. hydrophylacea* and *Coffea canephora* (Figure S8). Thus, *Ks* distributions and collinearity patterns for paralogous genes indicate no recent WGD event in *S. hydrophylacea*.

Evolution and function of tandem gene duplications

In the absence of recent WGD or large-scale gene duplications, we observed that TDs contributed to 56.1% of the gene family expansion in *S. hydrophylacea* (Figure 3a). We further compared the proportion of TDs across published mangrove genomes and found that mangroves without recent WGD had 18.2% of genes as TDs, significantly higher than the 8.4% in those with WGD (Mann–Whitney *U* test, *P*-value = 2.0×10^{-3}) (Figure 3a). Among significantly expanded gene families, TDs accounted for an average of 63.5% in mangroves lacking recent WGD, significantly higher than the 49.8% in those with WGDs (Mann–Whitney *U* test, *P*-value = 3.6×10^{-2}; Figure 3a; Table S5). These findings suggested that TDs may serve as an important mechanism driving gene family rapid expansion in mangroves, regardless of the presence of WGDs.

We calculated the *Ks* between tandemly duplicated gene pairs and found that the peak period of the duplication events occurred shortly after the divergence between *S. hydrophylacea* and *Coffea canephora* (Figure 3b). GO enrichment analysis further revealed that tandemly duplicated genes were significantly enriched in functional categories such as cation transmembrane transport, response to hypoxia and decreased oxygen levels, reactive oxygen species (ROS) response, hormone regulation, and calcium-mediated signaling (Figure 3c; Figure S9). The enrichment of these functions suggests that TDs may facilitate mangrove adaptation by enhancing stress tolerance, ion regulation, calcium signaling, oxygen sensing, and oxidative stress management for mangrove survival in intertidal environments.

We further validated this hypothesis using RNA-seq data collected under different salinity or waterlogging conditions (Materials and methods). In three salinity conditions, differentially expressed genes (DEGs) were identified when salt concentration increased from low to medium ($Salt_{(L\rightarrow M)}$) and from medium to high ($Salt_{(M\rightarrow H)}$). Similarly, for waterlogging treatments, DEGs were identified between 0 and 3 h ($Water_{(0h\rightarrow 3h)}$) and between 3 and 6 h of waterlogging ($Water_{(3h\rightarrow 6h)}$). In total, we identified 2165, 3198, and 4137 salt-responsive DEGs in leaf, root, and stem tissues, respectively, and 3745, 1313, and 1046 waterlogging-responsive DEGs in the corresponding tissues. We then found that during the $Salt_{(L\rightarrow M)}$ phase, DEGs in both leaf and root tissues were significantly enriched for TDs (*P*-values: 6.27×10^{-7} and 3.49×10^{-26}, respectively), whereas in $Salt_{(M\rightarrow H)}$ phase, such enrichment was observed in root tissue (*P*-value = 4.13×10^{-22}). When facing waterlogging stress, DEGs in leaf tissue showed significant TD enrichment during the $Water_{(0h\rightarrow 3h)}$ phase (*P*-value = 3.10×10^{-3}), while in the $Water_{(3h\rightarrow 6h)}$ phase, enrichment occurred in root tissue (*P*-value = 5.44×10^{-12}) (Figure 3d; Table S6). The overrepresentation of TDs among salt- and waterlogging-responsive genes supports the notion that TDs play a critical role in stress adaptation.

Tandem gene duplication and mechanisms of salt tolerance in *S. hydrophylacea*

Function annotation of TDs suggests that they are widely responsive to salt stress. We identified a series of gene family expansions potentially linked to high-salinity tolerance in *S. hydrophylacea*, which were further confirmed by transcriptome data across different salt conditions (Figures S10 and S11). The salt-responsive DEGs are enriched in biological processes such as "response to salt stress", "response to abscisic acid" and "response to water deprivation" (Figure S11). Similar GO term enrichments have been reported in other halophytes such as *Spartina alterniflora* (Huang et al., 2024) and *Tamarix chinensis* (Zhang et al., 2025).

One primary strategy for salt accumulation in *S. hydrophylacea* involves selective ion uptake and transport, mediated by transporters, such as HKT1, SOS, and NHX proteins. These transporters regulate sodium (Na^+), potassium (K^+), and chloride (Cl^-) ions to maintain ionic homeostasis. Excess ions are often sequestered into vacuoles via tonoplast-localized antiporters, such as NHX-type transporters, reducing cytoplasmic toxicity while maintaining osmotic balance. Notable expansions and differential gene expression were concentrated in cation and transmembrane transport (Figure 4; Figure S12). For instance, the *High-Affinity K^+ Transporter 1* (*HKT1*), a gene encoding K^+/Na^+ transmembrane transporter, expanded to eight copies in *S. hydrophylacea*. This is notably higher than the 1–3 copies found in inland relatives and some halophytes (Figure 4a). These expanded copies maintain the complete cation transport domain and exhibit comparable *Ka/Ks* ratios to homologs in other species, indicating preserved

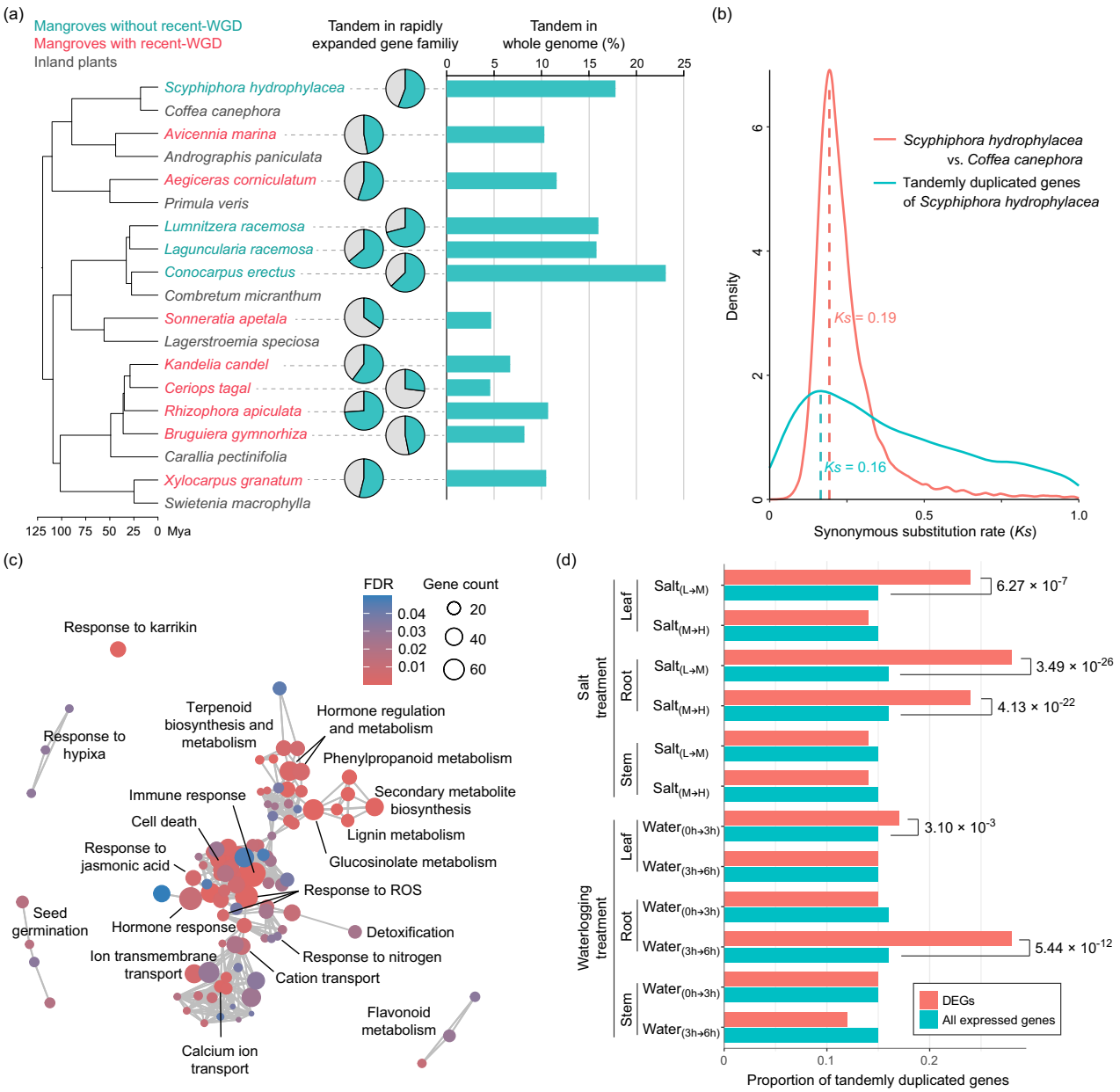

Figure 3. Evolution and function of tandem gene duplications.
(a) Contribution of tandem gene duplications to gene family expansion in mangroves with or without WGD events. The central pie chart shows the proportion of rapidly expanding gene families driven by TD, while the bar chart displays the proportion of tandemly duplicated genes in each mangrove clade.
(b) *Ks* distributions for tandemly duplicated paralogs in *S. hydrophylacea* and orthologs between *S. hydrophylacea* and *Coffea canephora*.
(c) Overrepresented GO terms for biological processes among tandemly duplicated gene families in *S. hydrophylacea*. Bubble size and color indicate gene numbers and false discovery rate (FDR), respectively (Fisher's exact test, Benjamini–Hochberg correction).
(d) Preferential expression patterns of tandemly duplicated genes in response to increasing stress intensity. Significance was assessed using Fisher's exact test. The red bars represent the proportion of tandemly duplicated genes (TDs) among differentially expressed genes (DEGs) in each tissue under defined phases. The cyan bars represent the proportion of TDs among all expressed genes in each tissue under the same phase. The numbers on the right side of the bars indicate the significance *P*-values.

biological function (Table S7). Phylogenetic analysis of the *HKT1* gene family revealed two duplication events: one at the most recent common ancestor (MRCA) of Gentianales and Solanales, and another at the MRCA of Rubiaceae (Figure S12). The duplicated copies exhibited functional divergence, with four copies mainly induced in root and the other four copies induced in leaf or stem (Figure 4b).

The *Auto-Inhibited Ca^{2+}-ATPase 12* (*ACA12*) gene family, which regulates cytosolic Ca^{2+} levels as a key second messenger in abiotic stress responses, has expanded to 13

copies in *S. hydrophylacea*, whereas inland relatives have only 0–6 copies (Figure 4a). *ACA12* was significantly upregulated under high salt conditions (Figure 4b). Genes involved in Na^+ transport from cytoplasm to vacuole, such as *H^+-ATPase* and *NHX*, were also upregulated with increasing salt concentration (Figure 4c). This upregulation may enhance salt transport efficiency from the cytoplasm to the vacuole in mesophyll cells (Figure 4c).

High salinity also disrupts osmotic balance, leading to denaturation and inactivation of intracellular proteins. In *S. hydrophylacea*, the *Polyol/Monosaccharide Transporter 1/2* (*PMT1/2*) gene, which is involved in polyol transport, has expanded to 10 copies, compared with 1–3 copies in inland relatives (Figure 4a). Additionally, *HSP20 Class CI* (*HSP20-CI*) gene and *Osmotin 34* (*OSM34*) gene, which act as molecular chaperones to protect protein folding under stress, have expanded to 17 and 16 copies in *S. hydrophylacea*, in contrast to 11 and 7 copies in *C. canephora*, and 6 and 1 copies in *Arabidopsis thaliana*. *OSM34*, *PMT1/2*, and *HSP20-CI* genes were all upregulated under high salt conditions, highlighting their roles in stress adaptation (Figure 4b,c).

High salinity often induces reactive oxygen species (ROS) accumulation, leading to cellular damage. To mitigate ROS toxicity, plants activate antioxidant defense mechanisms, including key enzymes such as superoxide dismutase (SOD), catalase, and peroxidases (PER). Additionally, secondary metabolites, such as glutathione, flavonoids, anthocyanins, polyphenolics, and carotenoids are accumulated. In *S. hydrophylacea*, several ROS-scavenging gene families have undergone expansions, with *Glutathione S-transferases* (*GSTs*) expanding to 19 copies, compared with seven in *A. thaliana*; *Rare Cold Inducible Gene 3* (*RCI3*) expanding to four copies, compared with only one copy in most mangrove species, three in *A. thaliana*, and 1–2 in other Gentianales species; and *Laccase 14/15* (*LAC14/15*) expanding to 13 copies, compared with two in *A. thaliana* and 3–6 in other Gentianales species (Figure 4a). Consistent with the extensive tandem gene duplication, genes involved in antioxidant biosynthesis, including glutathione, flavonoid, SOD, and PER, were significantly upregulated, contributing to ROS scavenging and mitigation of secondary oxidation stress induced by salt (Figure 4c). Transcription factors such as WRKY and AP2/ERF, which regulate flavonoid biosynthesis and glutathione metabolism (Mizoi *et al.*, 2012; Jiang et al., 2017), were also significantly upregulated (Figure 4b,c).

Tandem gene duplications contribute to hypoxia tolerance in *S. hydrophylacea*

Waterlogging is another major challenge for mangroves, causing hypoxia in roots. Despite lacking specialized aerial roots for gas exchange, *S. hydrophylacea* exhibits notable waterlogging tolerance (Figures S1 and S2). Transcriptome sequencing revealed that waterlogging-responsive DEGs are enriched in biological processes such as "carbohydrate metabolic process", "cell wall organization or biogenesis" and "response to oxidative stress" (Figure 5a). These expression patterns are consistent with responses observed in other wetland or aquatic species, such as bald-cypress *Taxodium distichum* (Yang et al., 2025) and *Nymphoides peltata* (Wu et al., 2017).

To survive under hypoxic or anoxic conditions, plants shift from aerobic respiration to fermentation to generate ATP and recycle NAD. In *S. hydrophylacea*, genes involved in sucrose metabolism, glycolysis, and fermentation underwent TDs and were upregulated under waterlogging conditions. Under anoxic conditions, sucrose is cleaved principally by sucrose synthase rather than invertase to produce more ATP. The *Sucrose Synthase* (*SUSs*) and *UDP-glucose Pyrophosphorylase* (*UGP*) in this process are upregulated. Nearly, all glycolysis-related genes were upregulated, except *Phosphoglucomutase* (*PGM*) and *Triosephosphate Isomerase* (*TPI*), which maintained consistently high expression levels (Figure 5c). Pyruvate, the final product of glycolysis, then enters the ethanol fermentation pathway. Genes encoding key enzymes in this pathway, including *Alcohol Dehydrogenase 1* (*ADH1*), *Pyruvate Decarboxylase* (*PDC*) and *Alanine Aminotransferase* (*AlaAT*), are upregulated in waterlogging conditions (Figure 5c). Especially, *ADH1* has undergone TDs, and all copies resulting from the duplication have shown significant upregulation in expression.

Hypoxia signal transduction and activation of downstream responses need the ethylene response factor 7 (ERF7) transcription factors. In *S. hydrophylacea*, the *ERF7* gene family expanded to eight copies through TDs, compared with 1–3 copies in inland relatives (Figure 5c). These duplications occurred 18–10 Mya and coincided with the period of inhabiting intertidal zones of *S. hydrophylacea* (Figure S13). [Correction added on 05 September 2025, after first online publication: In the above sentence the time period '18–100 Mya' has been corrected to '18–10 Mya'.] Sequence evolution analyses, protein domain annotations, and expression profiles confirm that all eight copies retain biological functions (Figure 5b; Table S8). These eight *ERF7* genes are mainly functionally active in root tissues. Additionally, increased expression of *PGB* inhibited ERF7 degradation, enabling greater accumulation of ERF7 in the cytoplasm and its subsequent nuclear translocation. Genes encoding plant cysteine oxidases (PCOs) enzymes that oxidize the penultimate cysteine of ERF7 also experienced duplication and exhibited increased expression (Figure 5c).

Waterlogging-induced hypoxia also leads to ROS accumulation and protein misfolding. To mitigate oxidative stress, *S. hydrophylacea* exhibited TDs and upregulation of antioxidant-related genes, including *Glutathione S-transferases* (*GSTs*), *Glutathione Peroxidase* (*GPX*), and

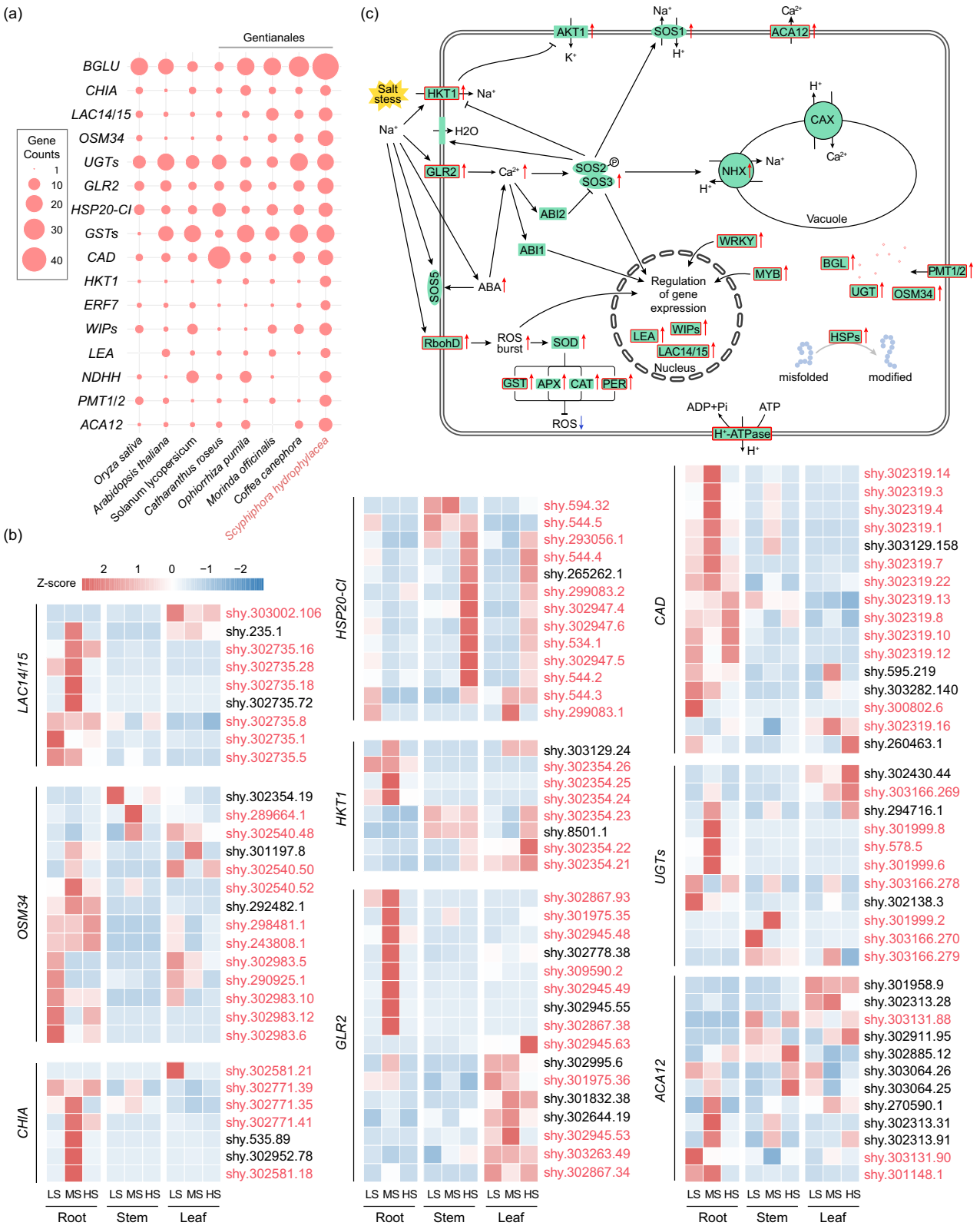

Peroxidase (*PER*), which function in ROS scavenging (Figure 5c). *Heat Shock Proteins* (*HSPs*) were also strongly upregulated, ensuring proper protein folding under stress conditions. Additionally, several hypoxia-responsive genes classified as *Hypoxia Response Unknown Proteins* (*HUPs*) underwent TDs and were upregulated. Among them,

Figure 4. Tandem gene duplication and salt response in *S. hydrophylacea*.
(a) Expansion of salt-responsive genes in *S. hydrophylacea*. Bubble size indicates gene copy numbers.
(b) Expression profiles of salt-related tandemly duplicated genes (red names) under varying salinity conditions (LS: low salinity, MS: medium salinity, HS: high salinity). Gene TPM expressions are normalized using the Z-score among three tissues.
(c) Proposed salt accumulation pathway in *S. hydrophylacea* (adapted from Türkan & Demiral, 2009). Red upward arrows indicate genes upregulated under high salinity, while red outlines highlight genes expanded via tandem duplication. *ACA12*, auto-inhibited Ca^{2+} ATPase 12; *BGLU*, beta-glucosidase; *CAD*, cinnamyl alcohol dehydrogenase; *CHIA*, chitinase A; *ERF7*, ethylene response factor 7; *GLR2*, glutamate receptor Clade II; *GST*, glutathione S-transferase; *HKT1*, high-affinity K^+ transporter; *HSPs*, heat shock proteins; *LAC14/15*, Laccase 14/15; *LEA*, late embryogenesis abundant protein; *NDHH*, NAD(P)H dehydrogenase subunit H; *OSM34*, Osmotin 34; *PMT1/2*, polyol/monosaccharide transporter 1/2; *UGTs*, UDP-glycosyltransferases; *WIPs*, wound-induced polypeptides.

Wound-Induced Polypeptides (*WIPs*), encoding a zinc finger transcription factor involved in photomorphogenesis, flavonoid biosynthesis, and root development, expanded to 11 copies in *S. hydrophylacea*, compared with 1–8 copies in terrestrial species (Figure 4a). Overall, the extensive TD and upregulation of genes involved in fermentation metabolism, transcriptional regulation, ROS scavenging, and protein stability likely contribute to the enhanced hypoxia tolerance of *S. hydrophylacea*, supporting its adaptation to waterlogged intertidal environments.

DISCUSSION

Mangrove plants have repeatedly evolved from inland ancestors and acquired unique adaptations to the intertidal zone, an environment marked by high salinity and low oxygen availability. However, *S. hydrophylacea* represents an atypical case, exhibiting strong environmental tolerance without apparent morphological specializations. Our genome-wide analyses revealed that this adaptation is not associated with recent WGDs but is instead primarily driven by tandem gene duplications (TDs). The TDs predominantly occurred during the species' occupation of intertidal habitats and led to significant expansion of gene families directly involved in salt and hypoxia tolerance. The results suggest that the targeted expansion of functional gene families via TDs may represent an efficient strategy for rapid adaptation to extreme environments in this atypical mangrove. Overall, our findings highlight the evolutionary flexibility of TDs as a mechanism of niche adaptation.

Climate optimum promoted the mangrove origination

S. hydrophylacea originated ~18.1 Mya, coinciding with the Mid-Miocene Climatic Optimum (MMCO), a period from approximately 17 to 15 Mya characterized by significant increases in temperature and sea levels. Indeed, the origination during climatic optimum periods appears to be a universal phenomenon among mangroves. During the Paleocene–Eocene Thermal Maximum (PETM), another period of dramatic sea-level rise, three major mangrove clades—Rhizophoraceae, *Avicennia*, and *Sonneratia*—inhabited the intertidal zones (He et al., 2020; Xu et al., 2017). [Correction added on 05 September 2025, after first online publication: In the above sentence the word 'inhabited' was wrongly spelt and has been corrected in this version.] Furthermore, the divergence events within the largest mangrove clade, Rhizophoraceae, correlate with climate optimum events, specifically around 42 Mya and 15 Mya (He et al., 2022; Xu et al., 2024). These results suggest that the origin and spread of mangroves, including the atypical mangrove *S. hydrophylacea*, were largely driven by historical dramatic sea-level changes, which provided new ecological niches and opportunities for colonization.

Molecular mechanisms of salt and hypoxia tolerance of *S. hydrophylacea*

The most significant niche differences for mangroves that live in the intertidal zones are high salinity and periodic flooding compared with the terrestrial plants (Ball, 1988). Mangrove plants have developed several strategies to manage high salinity, including salt exclusion at root systems, salt secretion through specialized glands, salt translocation, and shedding of salt-saturated organs (Popp et al., 1993). Comparison analyses under salt stress suggested that *S. hydrophylacea* is a non-secretor and employs a strategy of transferring excess salt to leaves and storing it in vacuoles and later removing it through leaf drop (Cram et al., 2002; Wang et al., 2011). This process first requires transporting salt from the xylem into cells and accumulating it in vacuoles. Meanwhile, the vacuoles storing salt have relatively high osmotic pressure, so the plant needs to synthesize osmotic regulators such as betaine, prolines, and polyols, which balance cellular osmotic pressure and stabilize macromolecular structures under stress (Bhardwaj et al., 2013; Bose et al., 2014; Nouman et al., 2018; Singh et al., 2015). Additionally, the accumulated ROS and ions may affect protein conformation. Correspondingly, we observed a series of genes involved in these processes exhibited copy number expansion and upregulated expression in *S. hydrophylacea*. For example, a crucial step in Na^+ transport is unloading Na^+ from the xylem into cells, a process facilitated by the *HKT1* gene (Deinlein et al., 2014). In *S. hydrophylacea*, *HKT1* has expanded to eight copies, primarily due to TD. Most of these copies exhibit upregulated expression under increased salinity, potentially enhancing Na^+ unloading. The duplicated *HKT1* genes dominate different tissues, suggesting functional differentiation that allows more efficient and tissue-specific adaptation. Additionally, *HSP20-CI* shows significant upregulation in stems and leaves as salinity increases, which may help ensure proper protein folding and functionality during Na^+ accumulation.

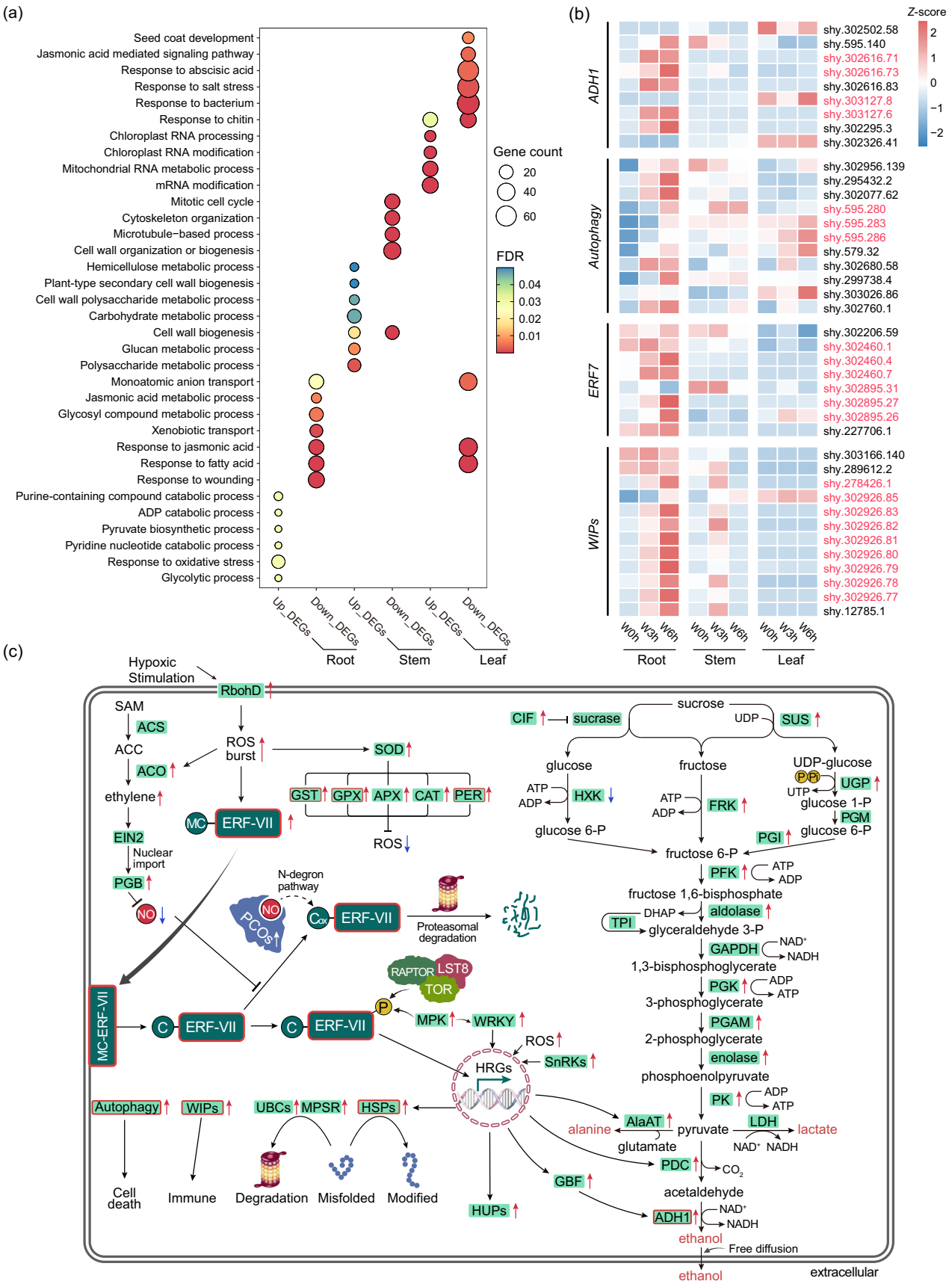

Figure 5. Tandem gene duplication and hypoxia tolerance in *S. hydrophylacea*.
(a) Overrepresented GO terms of differentially expressed genes under waterlogging treatment. Bubble size and color indicate gene numbers and FDR, respectively (Fisher's exact test, Benjamini–Hochberg correction). Up_DEGs and Down_DEGs refer to the upregulated and downregulated differentially expressed genes, respectively.
(b) Key hypoxia-tolerance pathway genes that underwent TD (red names) and responded to waterlogging (W0h: pre-waterlog, W3h: 3-h waterlog, W6h: 6-h waterlog). Gene TPM expressions are normalized using the *Z*-score among three tissues.
(c) Proposed hypoxia-response pathway in *S. hydrophylacea*. Red upward arrow indicates gene upregulated under hypoxia, while red outline highlights gene expanded via tandem duplication. *ACO*, ACC oxidase; *ACS*, ACC synthase; *ADH1*, alcohol dehydrogenase 1; *AlaAT*, alanine aminotransferase; *APX*, ascorbate peroxidase; *CAT*, catalase; *CIF*, cell wall/vacuolar inhibitor of fructosidase; *EIN2*, ethylene insensitive 2; *ERF7*, ethylene response factor 7; *FRK*, fructokinase; *GAPDH*, glyceraldehyde 3-phosphate dehydrogenase; *GBF*, G-Box binding factor; *GPX*, glutathione peroxidase; *GSTs*, glutathione S-transferase Tau; HRGs, hypoxia-response genes; *HSP*, heat shock protein; *HUP*, hypoxia response unknown protein; *HXK*, hexokinase; *LDH*, lactate dehydrogenase; *LST8*, lethal with Sec 13; *MPK*, mitogen-activated protein kinase; *MPSR*, misfolded protein aensing ring E3 ligase; *PCOs*, plant cysteine oxidases; *PDC*, pyruvate decarboxylase; *PER*, peroxidase; *PFK*, phosphofructokinase; *PGAM*, phosphoglycerate mutase; *PGB*, phytoglobin; *PGI*, phosphoglucose isomerase; *PGK*, phosphoglycerate kinase; *PGM*, phosphoglucomutase; *PK*, pyruvate kinase; *RbohD*, respiratory burst oxidase homolog D; *SnRK*, SNF1-related protein kinase; *SOD*, superoxide dismutase; *SUS*, sucrose synthase; *TOR*, target of rapamycin; *TPI*, triosephosphate isomerase; *UBC*, ubiquitin-conjugating enzyme; *UGP*, UDP-glucose pyrophosphorylase; *WIPs*, wound-induced polypeptides; *WRKY*, WRKY DNA-binding protein.

Waterlogging represents another major challenge for mangroves, leading to hypoxia in the root zones. *S. hydrophylacea* exhibits notable waterlogging tolerance (Guo et al., 2018; Wang, 2012). Our study suggests that *S. hydrophylacea* may have enhanced its response to hypoxia through tandem gene duplication. For instance, the transcription factor ERF7, which perceives hypoxia signals and activates downstream response genes, has undergone significant expansion through TD. These copies are highly expressed in roots, potentially strengthening the activation of hypoxia-response genes. Additionally, the key enzyme ADH1 in the anaerobic respiration pathway has expanded and is upregulated under waterlogging conditions. Therefore, the enhanced induction of responsive pathways by tandem expansion and upregulated expression may confer hypoxia tolerance to *S. hydrophylacea*.

The gene duplications identified in *S. hydrophylacea* are also observed in other mangroves (Figure 6). For example, the genes *HKT1* and *ERF7* exhibit increased copy numbers across nine independent mangrove clades compared with their inland relatives. The *HKT1* genes encode proteins that transport Na^+ into cells, and the *ERF7* genes encode transcription factors that mediate hypoxia signal transduction into the nucleus. These genes act as key hub genes in responses to high salinity and waterlogging, respectively (Deinlein et al., 2014; Mizoi et al., 2012; Wang et al., 2025; Yao et al., 2017). The gene *OSM34* and *HSP20-CI* that protect protein folding under stressful conditions have expanded exclusively in atypical mangroves that lack WGD events. This may be because the atypical mangroves have not evolved specialized traits to avoid adverse conditions and thus rely more heavily on these protective proteins. Additionally, genes such as *ADH1*, *ACA12*, *GLR2*, and *WIPs* show copy number expansion in at least two mangrove clades.

When examining other salt- and waterlogging-tolerant plants, we found that the expansions of *HKT1* and *ERF7* repeatedly occur. In halophytes *Thellungiella parvula* (Dassanayake et al., 2011), *Populus euphratica* (Ma et al., 2013), and *Cakile maritima* (Thomas et al., 2024), similar copy number expansion has been observed in *HKT1*. Seagrasses, including *Posidonia oceanica*, *Cymodocea nodosa*, *Zostera marina*, and *Thalassia testudinum*, have expanded the *ERF7* to 12–16 copies (Ma et al., 2024). In bald cypress that thrives in wetlands, *ERF7* has expanded to 24 copies (Yang et al., 2025). Notably, both genes have been mapped within salt- or waterlogging-related quantitative trait loci (QTLs) in various crops, including barley, wheat, maize, and rice (Chen et al., 2020; Houston et al., 2020; Hussain et al., 2017; Xu et al., 2006; Zhou et al., 2022), highlighting their potential as molecular targets for improving stress tolerance through breeding. These findings suggest that expansions of certain key stress-related genes may constitute a common strategy across multiple plants for coping with salt or hypoxia stress.

Tandem gene duplications dominate stress-responsive pathway modification

In *S. hydrophylacea*, the rapid expansion of genes related to salt and hypoxia tolerance has been achieved primarily through TDs. Indeed, many of the commonly observed gene duplications mentioned above experienced TDs, such as the *ERF7* in seagrasses and bald cypress. The expansions of *HKT1* in *Thellungiella parvula* and *Populus euphratica* are also achieved through TD. The TDs in *S. hydrophylacea* did not occur randomly, but are concentrated on processes related to stress response, such as cation transmembrane transport, ROS response, calcium-mediated signaling, immune response, and detection of oxygen/hypoxia. Although TDs may be generated continuously, the retained ones in *S. hydrophylacea* are mainly produced during the inhabitation of intertidal zones. Furthermore, without specialized traits to avoid the adverse conditions, atypical mangroves without WGDs could extensively duplicate the *OSM34* and *HSP20-CI* gene that protect protein folding through TDs (Figure 6). It supported the idea that TDs often target stress-responsive gene families, enabling more focused and flexible adaptation (Panchy et al., 2016).

Figure 6. Contribution of tandem gene duplications to salt/hypoxia-responsive gene expansions in mangroves with or without WGD events.
The species names are highlighted with green, red, and gray backgrounds, representing mangroves without recent WGD, mangroves with recent WGD, and inland relatives, respectively. In the bar plots, cyan and red are used to indicate tandem gene copies and non-tandem gene copies, respectively. *ACA12*, auto-inhibited Ca^{2+} ATPase 12; *ADH1*, alcohol dehydrogenase 1; *ERF7*, ethylene response factor 7; *GLR2*, glutamate receptor Clade II; *HKT1*, high-affinity K^{+} transporter 1; *HSP20-CI*, HSP20 Class CI chaperone families; *OSM34*, Osmotin 34; *WIPs*, wound-induced polypeptides.

Through their ability to introduce key regulatory or functional modifications with relatively small genomic changes, TD offers a powerful mechanism for generating genetic diversity and stress resilience traits critical for molecular breeding. Indeed, some of these TD-derived genes have already been mapped to key QTLs associated

with agronomic traits. In rice (*Oryza sativa* ssp. *indica* cultivar FR13A), *Sub1A*, a tandemly duplicated member of the *ERF* family, results in strong gene induction under submergence and significantly improved flooding tolerance (Xu et al., 2006). In the *Solanum* genus, TDs of the *CLV3* gene family generated redundant paralogs that fine-tune fruit development through dosage-sensitive interactions (Benoit et al., 2025). Similarly, in tomato, the fruit weight QTL *fw3.2* is linked to a TD of a *Cytochrome P450* gene, highlighting the role of TD-derived gene copies in regulating fruit size (Alonge et al., 2020). These TD-derived genes often maintain *cis*-regulatory conservation despite protein sequence divergence, suggesting a mechanism for rapid functional diversification under environmental pressures.

In summary, we explored the molecular basis required for plant intertidal adaptation with a high-quality genome assembly of an atypical mangrove *S. hydrophylacea*. Through comparative genomics and transcriptome analyses, we found that widespread tandem gene duplications significantly contribute to the adaptation of atypical mangroves by expanding essential genes associated with salt and hypoxia tolerance. These results underscore the crucial role of TDs as a primary genetic mechanism driving adaptation to extreme intertidal environments. The identified genetic variation in *S. hydrophylacea*, which specifically enhanced salt and hypoxia responses without changing phenotypes, may also serve as potential targets for crop breeding.

MATERIALS AND METHODS

Sampling and sequencing

Fresh and healthy leaves from a mature *Scyphiphora hydrophylacea* individual were collected in the Bamenwan Mangrove Nature Reserve in Wenchang, Hainan, China. The samples were immediately frozen in liquid nitrogen and stored at −80°C in the laboratory. Genomic DNA for sequencing was then extracted using a modified CTAB method. To obtain a high-quality genome assembly, a multi-platform sequencing strategy integrating 10× Genomics linked reads, paired-end short-read sequencing, and Hi-C technology was employed. For 10× Genomics sequencing, the DNA integrity was first assessed via agarose gel electrophoresis and Thermo Nanodrop™ 1000 Spectrophotometer (Thermo Fisher Scientific, https://www.thermofisher.com/). Then long DNA fragments (>50 kb) were collected through PippinHT size selection for 10× Genomics library preparation. The prepared sequencing library was sequenced across two lanes using PE150 paired-end reads on a BGISEQ-500 platform (BGI, https://en.genomics.cn/). SOAPnuke v2.1.6 (Chen et al., 2018) was employed to filter out low-quality, adapter, N-containing, and polyA sequences. The paired-end reads using a small insert fragment library (200–400 bp) were sequenced for gap closing. To further improve the assembly, a Hi-C library was prepared from DNA extracted from leaf tissues following *in situ* cross-linking. The Hi-C library was sequenced using the BGISEQ-500 platform, and the reads were filtered with SOAPnuke. Genome size was estimated based on *K*-mer distribution analysis using Illumina short reads. *K*-mers were generated with a 21-nt length using Jellyfish v2.3.0 (Marçais & Kingsford, 2011), and the genome size was estimated with GCE v1.0.2 (Liu et al., 2013).

Genome assembly

Clean reads were assembled and scaffolded using Supernova v2.0.1 (Weisenfeld et al., 2017). The gaps in the initial genome assembly were closed using TGS-GapCloser v1.12 (Xu et al., 2020) with default parameters. HiC-Pro v3.0.0 (Servant et al., 2015) was employed to map the Hi-C clean reads to the gap-closed assembly, providing valid reads with contact information between sequences. Juicer v1.6 (Durand, Shamim, et al., 2016) was then used to map these valid reads back to the gap-closed assembly, generating a comparison file suitable for a 3D-DNA input format. A 3D-DNA *de novo* genome assembly pipeline (Dudchenko et al., 2017) was executed using the results from Juicer as input. This process resulted in a patched genome assembled at the pseudochromosome level. The Hi-C file generated by 3D-DNA and the scaffold coordinate file were imported into JuiceBox v1.8.0 (Durand, Robinson, et al., 2016) to visualize fragmentation results. Based on the strength of the relationship between scaffolds, the positions and orientations of specific chromosome sequences were manually adjusted. The manually corrected scaffold coordinate file was re-imported into the 3D-DNA process. It rearranged the genome according to the updated coordinate file and connected it to the chromosome-level scaffolds, producing the final genome assembly. To evaluate the completeness of the genome assembly, we examined the existence of core eudicot gene sets using BUSCO v5.7.1 (Manni *et al.*, 2021) and calculated the mapping rate of sequencing reads to genome assembly using BWA v0.7.17 (Li & Durbin, 2009).

Genome annotation

We annotated repetitive elements in the *S. hydrophylacea* genome using a combined *de novo* and homology-based approach. First, we generated a *de novo* predicted repeat library using RepeatModeler v2.0.1 (https://www.repeatmasker.org/), which integrated the library Dfam v3.2 (https://www.dfam.org/) and library RepBase (v2018-10-26, https://www.girinst.org/). The resulting consensus library from RepeatModeler was then used with RepeatMasker v4.1.5 (A.F.A. Smit, R. Hubley & P. Green at https://repeatmasker.org/) to annotate and classify repetitive elements throughout the genome. With repetitive sequences masked, structures of protein-coding genes were predicted using a multi-faceted approach that integrated homology-based prediction, *de novo* prediction, and transcriptome-based prediction. Augustus v3.3.1 (Hoff & Stanke, 2019) and GlimmerHMM v3.0.4c (Majoros et al., 2004) were employed for *de novo* gene prediction. Homology-based prediction was performed using *Coffea canephora* and *Arabidopsis thaliana* as reference species, while transcriptome-based prediction was supported by RNA-seq data derived from root, stem, and leaf tissues of *S. hydrophylacea*.

Genome collinearity analysis

WGDs produce homologous genes within the same range, forming collinear blocks. Homologous genes were first identified using BLAST v2.12.0+ (Camacho et al., 2009) (with e-value $\leq 1 \times 10^{-10}$, identity score ≥40%). Then, collinear blocks were defined as genomic regions containing at least five homologous genes arranged in a conserved order across other genomic regions (Wang et al., 2012). Collinear blocks were visualized using Circos v0.69.9 and JCVI v1.4.16 (Krzywinski et al., 2009; Tang et al., 2008).

Synonymous substitution rate (*Ks*) between collinear gene pairs was calculated to estimate the time of WGDs. Protein alignment of the collinear gene pairs was first performed using MAFFT v7.475 (Katoh & Standley, 2013) in high-accuracy mode. Then,

PAL2NAL v14 (Suyama et al., 2006) was employed to convert the well-aligned protein sequences into corresponding codon alignments. After removing codons with gaps, the *Ks* for each homologous pair was calculated using KaKs_Calculator v2.0 (Wang et al., 2010) with the YN model (Yang & Nielsen, 2000).

Phylogeny and divergence time estimation

A phylogenetic tree was reconstructed using single-copy orthologous genes from *S. hydrophylacea* and eight additional species, including *Coffea canephora* (Denoeud et al., 2014), *Morinda officinalis* (Wang et al., 2021), *Ophiorrhiza pumila* (Rai et al., 2021), *Catharanthus roseus* (Franke et al., 2019), *Solanum lycopersicum* (Hosmani et al., 2019), *Arabidopsis thaliana* (Cheng et al., 2017), *Nelumbo nucifera* (Li et al., 2021), *Oryza sativa* (Ouyang et al., 2007). For genes with alternative splicing, only the longest transcript was retained. After excluding short proteins (≤50 amino acids), OrthoFinder v2.5.2 (Emms & Kelly, 2019) was used to identify single-copy orthologs among the nine species (with *e*-value $\leq 1 \times 10^{-10}$ and identity score ≥40%).

Protein alignments of these single-copy orthologs were first generated using MAFFT in high-accuracy mode. The well-aligned protein sequences were then converted into corresponding codon alignments using PAL2NAL. Gblocks v0.91b (Castresana, 2000) was employed with the parameters of "-t=c, -b4=10, -b5=h" to eliminate the poorly aligned positions and divergent regions of the alignment sequences. The best nucleotide mutation model was selected through ModelTest-NG v0.1.7 (Darriba et al., 2020). The maximum likelihood tree was constructed using RaxML-NG v1.0.2 (Kozlov et al., 2019). To estimate species divergence times, we utilized MCMCTREE of PAML v4.9j (Yang, 2007), incorporating two reliable calibration points: the MRCA of Proteales and core eudicots (119.6–128.63 Mya) (Morris et al., 2018), and the crown node of the Gentianales (72.5–97.6 Mya) (Kumar et al., 2017).

Gene family evolution

We calculated the gene family counts of the nine species using OrthoFinder v2.5.2, excluding large gene families with more than 100 gene copies in one or more species. CAFE v4.2.1 (De Bie et al., 2006) was used to identify significantly expanded/contracted gene families (*P*-value <0.01). Gene ontology (GO) enrichment and KEGG pathway analyses on the expanded gene families were conducted using the R package clusterProfiler v4.1.3 (Wu et al., 2021).

The identified gene family expansions were further validated through domain search and phylogenetic tree construction. Domains were identified by searching against the Pfam database (Mistry et al., 2021) using HMMER v3.4 (Eddy, 2011). The domains include PF00314 (Thaumatin family domain; for *OSM34*), PF00011 (Alpha crystallin/Hsp20 domain; for *HSP20-Cl*), PF00107 (Alcohol dehydrogenase-like, C-terminal domain; for *ADH1*), PF08240 (Alcohol dehydrogenase, N-terminal domain; for *ADH1*), PF00122 (E1-E2 ATPase domain; for *ACA12*), PF02386 (Cation transporter domain; for *HKT1*), PF00847 (AP2/ERF domain; for *ERF7*), PF00060 (Ligand-gated ion channel domain; for *GLR2*), and PF12609 (Wound-induced Protein domain; for *WIPs*).

Tandem gene duplication identification

Tandem gene duplications (TDs) were identified as paralogous genes in one gene family located within the same or neighboring intergenic regions, with no more than five intervening genes. The distribution of synonymous substitution rates (*Ks*) between copies from a TD cluster was estimated using KaKs_Calculator v2.0 to estimate the timing of TD events. GO enrichment analyses of TDs were conducted using the R package clusterProfiler v4.1.3. Subsequently, the "emapplot" diagram of the R package was used to visualize the relationships and interactions among the significantly enriched GO terms.

Transcriptome sequencing and analyses

We conducted field sampling in the Qingmeigang Mangrove Nature Reserve in Hainan, China to investigate the transcriptional response of *S. hydrophylacea* under natural salinity and waterlogging conditions. For the salinity gradient experiment, samples were collected from three distinct field locations where the ambient soil salinity levels, measured at the time of sampling, were naturally <10‰ (low-salinity group, LS), 35‰–40‰ (medium-salinity group, MS), and 45‰–50‰ (high-salinity group, HS). For the waterlogging experiment, we utilized the natural tidal cycle, during which the root systems of *S. hydrophylacea* were submerged for approximately 6 h. Based on this ecological context, tissue samples were collected at three time points: prior to waterlogging (W0h), after 3 h of waterlogging (W3h), and after 6 h of waterlogging (W6h). For each salinity or waterlogging condition, leaf, stem, and root tissues were collected. To minimize gene expression variation among individual plants, each sample contained three biological replicates.

All samples were immediately frozen in liquid nitrogen on-site and subsequently transported under dry ice to the laboratory for RNA extraction. Total RNA was extracted using a modified CTAB method for transcriptome sequencing. RNA-seq libraries were prepared and sequenced on the Illumina NovaSeq6000 platform, generating 150-bp paired-end reads. After filtering out low-quality reads, the clean data from each sample were mapped to the *S. hydrophylacea* genome using HISAT2 v2.2.1 (Kim *et al.*, 2019). The number of reads mapped to each gene was quantified using the featureCounts function in the R package Rsubread v2.14.2 (Liao et al., 2019).

Differential expression analyses among different salt or waterlogging conditions were performed using the Perl script "*run_DE_analysis.pl*" in Trinity v2.14.0 (Grabherr et al., 2011) with FDR <0.05 and a fold-change >2 or <0.5 considered as criteria for a significantly upregulated or downregulated gene. Gene expression levels were reported as transcripts per million (TPM). Key gene expression profiles were visualized using the R package pheatmap v1.0.12 (https://cran.r-project.org/package=pheatmap) with *Z-score* normalization applied between different tissues.

AUTHOR CONTRIBUTIONS

SX and SS conceived and designed the research. YW, YL, and ML collected materials. CJ, YL, and ML performed the experiments. YL and SX carried out data processing and analyses. YL and YW drew the pictures. YL and SX wrote the first draft of the manuscript. SX, SS, RZ, KH, ZG, ZH, and SS revised the manuscript. All authors have read and agreed to the published version of the manuscript.

ACKNOWLEDGMENTS

We thank Chung-I Wu from Sun Yat-sen University for the helpful discussion. We thank Ying Zhang from Lingnan Normal University for field assistance with sample collection. This study was supported by the National Natural Science Foundation of China (32370227 and 32330005).

CONFLICTS OF INTEREST

The authors declare no conflicts of interest.

DATA AVAILABILITY STATEMENT

The chromosome-level genome assembly of *Scyphiphora hydrophylacea* reported in this study has been deposited into CNGB Sequence Archive (CNSA) of China National GeneBank DataBase (CNGBdb, https://db.cngb.org/) with accession number CNP0005380. The genome assembly and annotations data can also be found at Figshare (https://doi.org/10.6084/m9.figshare.27021523). RNA sequencing data of salt and hypoxia treatment experiments also have been deposited in CNSA under accession CNP0005380.

SUPPORTING INFORMATION

Additional Supporting Information may be found in the online version of this article.

Figure S1. The largest *Scyphiphora hydrophylacea* community in China (Qingmeigang Mangrove Nature Reserve, Hainan).

Figure S2. *K*-mer frequency distribution of *S. hydrophylacea* sequencing reads.

Figure S3. Genomic architecture and completeness evaluation of *S. hydrophylacea*.

Figure S4. Unique and shared function annotations of *S. hydrophylacea* protein-coding genes using varying databases.

Figure S5. Gene Ontology (GO) categories of the protein-coding genes in *S. hydrophylacea*.

Figure S6. GO enrichment in biological process of 318 significantly expanded gene families in *S. hydrophylacea*.

Figure S7. KEGG pathway analysis of the 318 significantly expanded gene families of *S. hydrophylacea*.

Figure S8. Collinearity between *Scyphiphora hydrophylacea* and *Coffea canephora* revealed by chromosomal dot plots.

Figure S9. GO enrichment analysis of tandemly duplicated gene families in *S. hydrophylacea*.

Figure S10. The number of differentially expressed genes in three different tissues under salt or waterlogging.

Figure S11. GO enrichment in biological process of differentially expressed genes under salt stress.

Figure S12. Time tree of *HKT1* gene family.

Figure S13. Time tree of *ERF7* gene family.

Table S1. Raw sequencing data of *Scyphiphora hydrophylacea*.

Table S2. Information of the 11 pseudo-chromosomes assembly of *S. hydrophylacea*.

Table S3. Summary statistics of *S. hydrophylacea* genome assembly and annotation.

Table S4. The repetitive sequences of the *S. hydrophylacea* genome.

Table S5. Contribution of tandemly duplicated genes to rapidly expanded gene families among different mangrove clades.

Table S6. Preferential expression responses of tandemly duplicated genes in different tissues under salt and waterlogging conditions.

Table S7. Functional domain integrity prediction of *HKT1* gene family.

Table S8. Functional domain integrity prediction of *ERF7* gene family.

REFERENCES

Adams, K.L. & **Wendel, J.F.** (2005) Polyploidy and genome evolution in plants. *Current Opinion in Plant Biology*, **8**, 135–141.

Almeida-Silva, F. & **Van de Peer, Y.** (2023) Whole-genome duplications and the long-term evolution of gene regulatory networks in angiosperms. *Molecular Biology and Evolution*, **40**, msad141.

Alonge, M., Wang, X., Benoit, M., Soyk, S., Pereira, L., Zhang, L. *et al.* (2020) Major impacts of widespread structural variation on gene expression and crop improvement in tomato. *Cell*, **182**, 145–161.e23.

Ball, M.C. (1988) Ecophysiology of mangroves. *Trees*, **2**, 129–142.

Benoit, M., Jenike, K.M., Satterlee, J.W., Ramakrishnan, S., Gentile, I., Hendelman, A. *et al.* (2025) *Solanum* pan-genetics reveals paralogues as contingencies in crop engineering. *Nature*, **640**, 135–145.

Bhardwaj, R., Sharma, I., Kanwar, M., Sharma, R., Handa, N., Kaur, H. *et al.* (2013) LEA proteins in salt stress tolerance. In: *Salt Stress in Plants*. New York: Springer New York, pp. 79–112.

Bose, J., Rodrigo-Moreno, A. & **Shabala, S.** (2014) ROS homeostasis in halophytes in the context of salinity stress tolerance. *Journal of Experimental Botany*, **65**, 1241–1257.

Camacho, C., Coulouris, G., Avagyan, V., Ma, N., Papadopoulos, J., Bealer, K. *et al.* (2009) BLAST+: architecture and applications. *BMC Bioinformatics*, **10**, 421.

Castresana, J. (2000) Selection of conserved blocks from multiple alignments for their use in phylogenetic analysis. *Molecular Biology and Evolution*, **17**, 540–552.

Chen, C., Norton, G.J. & **Price, A.H.** (2020) Genome-wide association mapping for salt tolerance of rice seedlings grown in hydroponic and soil systems using the Bengal and Assam Aus panel. *Frontiers in Plant Science*, **11**, 576479.

Chen, Y., Chen, Y., Shi, C., Huang, Z., Zhang, Y., Li, S. *et al.* (2018) SOAPnuke: a MapReduce acceleration-supported software for integrated quality control and preprocessing of high-throughput sequencing data. *GigaScience*, **7**, gix120.

Cheng, C., Krishnakumar, V., Chan, A.P., Thibaud-Nissen, F., Schobel, S. & **Town, C.D.** (2017) Araport11: a complete reannotation of the *Arabidopsis thaliana* reference genome. *The Plant Journal*, **89**, 789–804.

Conant, G.C. & **Wolfe, K.H.** (2008) Turning a hobby into a job: how duplicated genes find new functions. *Nature Reviews Genetics*, **9**, 938–950.

Cram, J.W., Torr, P.G. & **Rose, D.A.** (2002) Salt allocation during leaf development and leaf fall in mangroves. *Trees*, **16**, 112–119.

Darriba, D., Posada, D., Kozlov, A.M., Stamatakis, A., Morel, B. & **Flouri, T.** (2020) ModelTest-NG: a new and scalable tool for the selection of DNA and protein evolutionary models. *Molecular Biology and Evolution*, **37**, 291–294.

Dassanayake, M., Oh, D.-H., Haas, J.S., Hernandez, A., Hong, H., Ali, S. *et al.* (2011) The genome of the extremophile crucifer *Thellungiella parvula*. *Nature Genetics*, **43**, 913–918.

De Bie, T., Cristianini, N., Demuth, J.P. & **Hahn, M.W.** (2006) CAFE: a computational tool for the study of gene family evolution. *Bioinformatics*, **22**, 1269–1271.

Deinlein, U., Stephan, A.B., Horie, T., Luo, W., Xu, G. & **Schroeder, J.I.** (2014) Plant salt-tolerance mechanisms. *Trends in Plant Science*, **19**, 371–379.

Denoeud, F., Carretero-Paulet, L., Dereeper, A., Droc, G., Guyot, R., Pietrella, M. *et al.* (2014) The coffee genome provides insight into the convergent evolution of caffeine biosynthesis. *Science*, **345**, 1181–1184.

Dudchenko, O., Batra, S.S., Omer, A.D., Nyquist, S.K., Hoeger, M., Durand, N.C. *et al.* (2017) De novo assembly of the *Aedes aegypti* genome using Hi-C yields chromosome-length scaffolds. *Science*, **356**, 92–95.

Duke, N.C. (2013) World Mangrove ID: expert information at your fingertips, App Store Version 1.1 for iPhone and iPad, Dec 2013. MangroveWatch Publication. e-book.

Durand, N.C., Robinson, J.T., Shamim, M.S., Machol, I., Mesirov, J.P., Lander, E.S. *et al.* (2016) Juicebox provides a visualization system for Hi-C contact maps with unlimited zoom. *Cell Systems*, **3**, 99–101.

Durand, N.C., Shamim, M.S., Machol, I., Rao, S.S.P., Huntley, M.H., Lander, E.S. *et al.* (2016) Juicer provides a one-click system for analyzing loop-resolution Hi-C experiments. *Cell Systems*, **3**, 95–98.

Eddy, S.R. (2011) Accelerated profile HMM searches. *PLoS Computational Biology*, **7**, e1002195.

Elmqvist, T. & **Cox, P.A.** (1996) The evolution of vivipary in flowering plants. *Oikos*, **77**, 3–9.

Emms, D.M. & **Kelly, S.** (2019) OrthoFinder: phylogenetic orthology inference for comparative genomics. *Genome Biology*, **20**, 238.

Feng, X., **Chen, Q.**, **Wu, W.**, **Wang, J.**, **Li, G.**, **Xu, S.** ***et al.*** (2024) Genomic evidence for rediploidization and adaptive evolution following the whole-genome triplication. *Nature Communications*, **15**, 1635.

Feng, X., **Li, G.**, **Xu, S.**, **Wu, W.**, **Chen, Q.**, **Shao, S.** ***et al.*** (2021) Genomic insights into molecular adaptation to intertidal environments in the mangrove *Aegiceras corniculatum*. *New Phytologist*, **231**, 2346–2358.

Franke, J., **Kim, J.**, **Hamilton, J.P.**, **Zhao, D.**, **Pham, G.M.**, **Wiegert-Rininger, K.** ***et al.*** (2019) Gene discovery in *Gelsemium* highlights conserved gene clusters in monoterpene indole alkaloid biosynthesis. *Chembiochem*, **20**, 83–87.

Giesen, W., **Wulffraat, S.**, **Zieren, M.** & **Scholten, L.** (2007) *Mangrove guidebook for Southeast Asia*. Bangkok: FAO Regional Office for Asia and the Pacific.

Goldner, A., **Herold, N.** & **Huber, M.** (2014) The challenge of simulating the warmth of the mid-Miocene climatic optimum in CESM1. *Climate of the Past*, **10**, 523–536.

Grabherr, M.G., **Haas, B.J.**, **Yassour, M.**, **Levin, J.Z.**, **Thompson, D.A.**, **Amit, I.** ***et al.*** (2011) Full-length transcriptome assembly from RNA-seq data without a reference genome. *Nature Biotechnology*, **29**, 644–652.

Guo, Z., **Li, X.**, **He, Z.**, **Yang, Y.**, **Wang, W.**, **Zhong, C.** ***et al.*** (2018) Extremely low genetic diversity across mangrove taxa reflects past sea level changes and hints at poor future responses. *Global Change Biology*, **24**, 1741–1748.

Hagolani, P.F., **Zimm, R.**, **Vroomans, R.** & **Salazar-Ciudad, I.** (2021) On the evolution and development of morphological complexity: a view from gene regulatory networks. *PLoS Computational Biology*, **17**, e1008570.

Hanada, K., **Zou, C.**, **Lehti-Shiu, M.D.**, **Shinozaki, K.** & **Shiu, S.H.** (2008) Importance of lineage-specific expansion of plant tandem duplicates in the adaptive response to environmental stimuli. *Plant Physiology*, **148**, 993–1003.

He, Z., **Feng, X.**, **Chen, Q.**, **Li, L.**, **Li, S.**, **Han, K.** ***et al.*** (2022) Evolution of coastal forests based on a full set of mangrove genomes. *Nature Ecology & Evolution*, **6**, 738–749.

He, Z., **Xu, S.**, **Zhang, Z.**, **Guo, W.**, **Lyu, H.**, **Zhong, C.** ***et al.*** (2020) Convergent adaptation of the genomes of woody plants at the land–sea interface. *National Science Review*, **7**, 978–993.

Hoff, K.J. & **Stanke, M.** (2019) Predicting genes in single genomes with AUGUSTUS. *Current Protocols in Bioinformatics*, **65**, e57.

Hosmani, P.S., **Flores-Gonzalez, M.**, **van de Geest, H.** ***et al.*** (2019) An improved *de novo* assembly and annotation of the tomato reference genome using single-molecule sequencing, Hi-C proximity ligation and optical maps. *bioRxiv*, 767764.

Houston, K., **Qiu, J.**, **Wege, S.**, **Hrmova, M.**, **Oakey, H.**, **Qu, Y.** ***et al.*** (2020) Barley sodium content is regulated by natural variants of the Na^+ transporter *HvHKT1;5*. *Communications Biology*, **3**, 258.

Huang, Z., **Chen, S.**, **He, K.**, **Yu, T.**, **Fu, J.**, **Gao, S.** ***et al.*** (2024) Exploring salt tolerance mechanisms using machine learning for transcriptomic insights: case study in *Spartina alterniflora*. *Horticulture Research*, **11**, uhae082.

Hussain, B., **Lucas, S.J.**, **Ozturk, L.** & **Budak, H.** (2017) Mapping QTLs conferring salt tolerance and micronutrient concentrations at seedling stage in wheat. *Scientific Reports*, **7**, 15662.

Jiang, J., **Ma, S.**, **Ye, N.**, **Jiang, M.**, **Cao, J.** & **Zhang, J.** (2017) WRKY transcription factors in plant responses to stresses. *Journal of Integrative Plant Biology*, **59**, 86–101.

Katoh, K. & **Standley, D.M.** (2013) MAFFT multiple sequence alignment software version 7: improvements in performance and usability. *Molecular Biology and Evolution*, **30**, 772–780.

Kim, D., **Paggi, J.M.**, **Park, C.**, **Bennett, C.** & **Salzberg, S.L.** (2019) Graph-based genome alignment and genotyping with HISAT2 and HISAT-genotype. *Nature Biotechnology*, **37**, 907–915.

Kozlov, A.M., **Darriba, D.**, **Flouri, T.**, **Morel, B.** & **Stamatakis, A.** (2019) RAxML-NG: a fast, scalable and user-friendly tool for maximum likelihood phylogenetic inference. *Bioinformatics*, **35**, 4453–4455.

Krzywinski, M., **Schein, J.**, **Birol, I.**, **Connors, J.**, **Gascoyne, R.**, **Horsman, D.** ***et al.*** (2009) Circos: an information aesthetic for comparative genomics. *Genome Research*, **19**, 1639–1645.

Kumar, S., **Stecher, G.**, **Suleski, M.** & **Hedges, S.B.** (2017) TimeTree: a resource for timelines, timetrees, and divergence times. *Molecular Biology and Evolution*, **34**, 1812–1819.

Li, H. & **Durbin, R.** (2009) Fast and accurate short read alignment with Burrows-Wheeler transform. *Bioinformatics*, **25**, 1754–1760.

Li, H., **Yang, X.**, **Zhang, Y.**, **Gao, Z.**, **Liang, Y.**, **Chen, J.** ***et al.*** (2021) *Nelumbo* genome database, an integrative resource for gene expression and variants of *Nelumbo nucifera*. *Scientific Data*, **8**, 38.

Liao, Y., **Smyth, G.K.** & **Shi, W.** (2019) The R package Rsubread is easier, faster, cheaper and better for alignment and quantification of RNA sequencing reads. *Nucleic Acids Research*, **47**, e47.

Liu, B., **Shi, Y.**, **Yuan, J.** ***et al.*** (2013) Estimation of genomic characteristics by analyzing *k*-mer frequency in *de novo* genome projects. *arXiv*, 1308.2012.

Ma, T., **Wang, J.**, **Zhou, G.**, **Yue, Z.**, **Hu, Q.**, **Chen, Y.** ***et al.*** (2013) Genomic insights into salt adaptation in a desert poplar. *Nature Communications*, **4**, 2797.

Ma, X., **Vanneste, S.**, **Chang, J.**, **Ambrosino, L.**, **Barry, K.**, **Bayer, T.** ***et al.*** (2024) Seagrass genomes reveal ancient polyploidy and adaptations to the marine environment. *Nature Plants*, **10**, 240–255.

Majoros, W.H., **Pertea, M.** & **Salzberg, S.L.** (2004) TigrScan and GlimmerHMM: two open source *ab initio* eukaryotic gene-finders. *Bioinformatics*, **20**, 2878–2879.

Manni, M., **Berkeley, M.R.**, **Seppey, M.**, **Simão, F.A.** & **Zdobnov, E.M.** (2021) BUSCO update: novel and streamlined workflows along with broader and deeper phylogenetic coverage for scoring of eukaryotic, prokaryotic, and viral genomes. *Molecular Biology and Evolution*, **38**, 4647–4654.

Marçais, G. & **Kingsford, C.** (2011) A fast, lock-free approach for efficient parallel counting of occurrences of *k*-mers. *Bioinformatics*, **27**, 764–770.

Medina-Gomez, C., **Lao, O.** & **Rivadeneira, F.** (2017) Evolution of complex traits in human populations. In: *Evolutionary biology: self/nonself evolution, species and complex traits evolution, methods and concepts*. Cham, Switzerland: Springer Nature, pp. 165–186.

Miller, K.G., **Browning, J.V.**, **Schmelz, W.J.**, **Kopp, R.E.**, **Mountain, G.S.** & **Wright, J.D.** (2020) Cenozoic sea-level and cryospheric evolution from deep-sea geochemical and continental margin records. *Science Advances*, **6**, eaaz1346.

Mimura, T., **Kura-Hotta, M.**, **Tsujimura, T.**, **Ohnishi, M.**, **Miura, M.**, **Okazaki, Y.** ***et al.*** (2003) Rapid increase of vacuolar volume in response to salt stress. *Planta*, **216**, 397–402.

Mistry, J., **Chuguransky, S.**, **Williams, L.**, **Qureshi, M.**, **Salazar, G.A.**, **Sonnhammer, E.L.L.** ***et al.*** (2021) Pfam: the protein families database in 2021. *Nucleic Acids Research*, **49**, D412–D419.

Mizoi, J., **Shinozaki, K.** & **Yamaguchi-Shinozaki, K.** (2012) AP2/ERF family transcription factors in plant abiotic stress responses. *Biochimica et Biophysica Acta (BBA) - Gene Regulatory Mechanisms*, **1819**, 86–96.

Morris, J.L., **Puttick, M.N.**, **Clark, J.W.**, **Edwards, D.**, **Kenrick, P.**, **Pressel, S.** ***et al.*** (2018) The timescale of early land plant evolution. *Proceedings of the National Academy of Sciences of the United States of America*, **115**, E2274–E2283.

Nouman, W., **Qureshi, M.K.**, **Shaheen, M.** & **Zubair, M.** (2018) Variation in plant bioactive compounds and antioxidant activities under salt stress. In: *Biotic and Abiotic Stress Tolerance in Plants*. Singapore: Springer Singapore, pp. 77–101.

Oh, D., **Hong, H.**, **Lee, S.Y.**, **Yun, D.**, **Bohnert, H.J.** & **Dassanayake, M.** (2014) Genome structures and transcriptomes signify niche adaptation for the multiple-ion-tolerant extremophyte *Schrenkiella parvula*. *Plant Physiology*, **164**, 2123–2138.

Ouyang, S., **Zhu, W.**, **Hamilton, J.**, **Lin, H.**, **Campbell, M.**, **Childs, K.** ***et al.*** (2007) The TIGR Rice genome annotation resource: improvements and new features. *Nucleic Acids Research*, **35**, D883–D887.

Panchy, N., **Lehti-Shiu, M.** & **Shiu, S.-H.** (2016) Evolution of gene duplication in plants. *Plant Physiology*, **171**, 2294–2316.

Parida, A.K. & **Jha, B.** (2010) Salt tolerance mechanisms in mangroves: a review. *Trees*, **24**, 199–217.

Plata, G., **Henry, C.S.** & **Vitkup, D.** (2015) Long-term phenotypic evolution of bacteria. *Nature*, **517**, 369–372.

Popp, M., **Polania, J.** & **Weiper, M.** (1993) Physiological adaptations to different salinity levels in mangrove. In: *Towards the rational use of high salinity tolerant plants*. Dordrecht: Springer, pp. 217–224.

Rai, A., **Hirakawa, H.**, **Nakabayashi, R.** ***et al.*** (2021) Chromosome-level genome assembly of *Ophiorrhiza pumila* reveals the evolution of camptothecin biosynthesis. *Nature Communications*, **12**, 1–19.

Reuter, M., **Harzhauser, M.** & **Piller, W.E.** (2021) The role of sea-level and climate changes in the assembly of Sri Lankan biodiversity: a perspective from the Miocene Jaffna Limestone. *Gondwana Research*, **91**, 152–165.

Servant, N., **Varoquaux, N.**, **Lajoie, B.R.**, **Viara, E.**, **Chen, C.-J.**, **Vert, J.-P.** ***et al.*** (2015) HiC-Pro: an optimized and flexible pipeline for Hi-C data processing. *Genome Biology*, **16**, 259.

Shi, S., **Huang, Y.**, **Zeng, K.**, **Tan, F.**, **He, H.**, **Huang, J.** ***et al.*** (2005) Molecular phylogenetic analysis of mangroves: independent evolutionary origins of vivipary and salt secretion. *Molecular Phylogenetics and Evolution*, **34**, 159–166.

Singh, M., **Kumar, J.**, **Singh, S.**, **Singh, V.P.** & **Prasad, S.M.** (2015) Roles of osmoprotectants in improving salinity and drought tolerance in plants: a review. *Reviews in Environmental Science and Bio/Technology*, **14**, 407–426.

Srikanth, S., **Lum, S.K.Y.** & **Chen, Z.** (2016) Mangrove root: adaptations and ecological importance. *Trees*, **30**, 451–465.

Sudhir, S., **Arunprasath, A.** & **Sankara Vel, V.** (2022) A critical review on adaptations, and biological activities of the mangroves. *Journal of Natural Pesticide Research*, **1**, 100006.

Suyama, M., **Torrents, D.** & **Bork, P.** (2006) PAL2NAL: robust conversion of protein sequence alignments into the corresponding codon alignments. *Nucleic Acids Research*, **34**, W609–W612.

Tang, H., **Bowers, J.E.**, **Wang, X.**, **Ming, R.**, **Alam, M.** & **Paterson, A.H.** (2008) Synteny and collinearity in plant genomes. *Science*, **320**, 486–488.

Thomas, S.K., **Vanden Hoek, K.**, **Ogoti, T.**, **Duong, H.**, **Angelovici, R.**, **Pires, J.C.** ***et al.*** (2024) Halophytes and heavy metals: a multi-omics approach to understand the role of gene and genome duplication in the abiotic stress tolerance of *Cakile maritima*. *American Journal of Botany*, **111**, e16310.

Tomlinson, P.B. (2016) *The botany of mangroves*. New York: Cambridge University Press.

Tsuda, K., **Itoigawa, J.** & **Yamanoi, T.** (1984) On the Middle Miocene palaeoenvironment of Japan with special reference to the ancient mangrove swamps. The Evolution of the East Asian Environment. 1. Geology and Palaeoclimatology.

Türkan, I. & **Demiral, T.** (2009) Recent developments in understanding salinity tolerance. *Environmental and Experimental Botany*, **67**, 2–9.

Wang, D., **Zhang, Y.**, **Zhang, Z.**, **Zhu, J.** & **Yu, J.** (2010) KaKs_Calculator 2.0: a toolkit incorporating gamma-series methods and sliding window strategies. *Genomics, Proteomics & Bioinformatics*, **8**, 77–80.

Wang, J., **Xu, S.**, **Mei, Y.**, **Cai, S.**, **Gu, Y.**, **Sun, M.** ***et al.*** (2021) A high-quality genome assembly of *Morinda officinalis*, a famous native southern herb in the Lingnan region of southern China. *Horticulture Research*, **8**, 135.

Wang, L., **Mu, M.**, **Li, X.**, **Lin, P.** & **Wang, W.** (2011) Differentiation between true mangroves and mangrove associates based on leaf traits and salt contents. *Journal of Plant Ecology*, **4**, 292–301.

Wang, L., **Wang, W.**, **Liao, K.**, **Xu, L.**, **Xie, D.**, **Xie, R.** ***et al.*** (2025) Survival mechanisms of plants under hypoxic stress: physiological acclimation and molecular regulation. *Journal of Integrative Plant Biology*, **67**, 440–454.

Wang, W. (2012) Investigation report on mangroves sudden dieback in Qingmeigang Nature Reserve, Sanya (in Chinese). *China Mangrove Conservation Network*, 1–36.

Wang, Y., **Tang, H.**, **DeBarry, J.D.**, **Tan, X.**, **Li, J.**, **Wang, X.** ***et al.*** (2012) MCScanX: a toolkit for detection and evolutionary analysis of gene synteny and collinearity. *Nucleic Acids Research*, **40**, e49.

Weisenfeld, N.I., **Kumar, V.**, **Shah, P.**, **Church, D.M.** & **Jaffe, D.B.** (2017) Direct determination of diploid genome sequences. *Genome Research*, **27**, 757–767.

Wu, H., **Zhang, Z.**, **Wang, J.**, **Wu, H.J.**, **Wang, J.Y.**, **Oh, D.H.** ***et al.*** (2012) Insights into salt tolerance from the genome of *Thellungiella salsuginea*. *Proceedings of the National Academy of Sciences of the United States of America*, **109**, 12219–12224.

Wu, J., **Zhao, H.-B.**, **Yu, D.** & **Xu, X.** (2017) Transcriptome profiling of the floating-leaved aquatic plant *Nymphoides peltata* in response to flooding stress. *BMC Genomics*, **18**, 119.

Wu, S., **Han, B.** & **Jiao, Y.** (2020) Genetic contribution of paleopolyploidy to adaptive evolution in angiosperms. *Molecular Plant*, **13**, 59–71.

Wu, T., **Hu, E.**, **Xu, S.**, **Chen, M.**, **Guo, P.**, **Dai, Z.** ***et al.*** (2021) clusterProfiler 4.0: a universal enrichment tool for interpreting omics data. *The Innovation*, **2**, 100141.

Xie, W., **Guo, Z.**, **Wang, J.**, **He, Z.**, **Li, Y.**, **Feng, X.** ***et al.*** (2023) Evolution of woody plants to the land-sea interface – the atypical genomic features of mangroves with atypical phenotypic adaptation. *Molecular Ecology*, **32**, 1351–1365.

Xu, K., **Xu, X.**, **Fukao, T.**, **Canlas, P.**, **Maghirang-Rodriguez, R.**, **Heuer, S.** ***et al.*** (2006) *Sub1A* is an ethylene-response-factor-like gene that confers submergence tolerance to rice. *Nature*, **442**, 705–708.

Xu, M., **Guo, L.**, **Gu, S.**, **Wang, O.**, **Zhang, R.**, **Peters, B.A.** ***et al.*** (2020) TGS-GapCloser: a fast and accurate gap closer for large genomes with low coverage of error-prone long reads. *GigaScience*, **9**, giaa094.

Xu, S., **Guo, Z.**, **Feng, X.**, **Shao, S.**, **Yang, Y.**, **Li, J.** ***et al.*** (2021) Where whole-genome duplication is most beneficial: adaptation of mangroves to a wide salinity range between land and sea. *Molecular Ecology*, **32**, 460–475.

Xu, S., **He, Z.**, **Zhang, Z.**, **Guo, Z.**, **Guo, W.**, **Lyu, H.** ***et al.*** (2017) The origin, diversification and adaptation of a major mangrove clade (Rhizophoreae) revealed by whole-genome sequencing. *National Science Review*, **4**, 721–734.

Xu, S., **Shao, S.**, **Feng, X.**, **Li, S.**, **Zhang, L.**, **Wu, W.** ***et al.*** (2024) Adaptation in unstable environments and global gene losses: small but stable gene networks by the May–Wigner theory. *Molecular Biology and Evolution*, **41**, msae059.

Yang, Y., **Yu, C.**, **Hua, J.**, **Wang, Z.**, **Chen, T.**, **Zhu, Q.** ***et al.*** (2025) The baldcypress genome provides insights into the adaptive evolution of flooding stress tolerance. *New Phytologist*, **247**, 979–997.

Yang, Z. (2007) PAML 4: phylogenetic analysis by maximum likelihood. *Molecular Biology and Evolution*, **24**, 1586–1591.

Yang, Z. & **Nielsen, R.** (2000) Estimating synonymous and nonsynonymous substitution rates under realistic evolutionary models. *Molecular Biology and Evolution*, **17**, 32–43.

Yao, Y., **He, R.**, **Xie, Q.**, **He, R.J.**, **Xie, Q.L.**, **Zhao, X.h.** ***et al.*** (2017) *ETHYLENE RESPONSE FACTOR 74* (*ERF74*) plays an essential role in controlling a respiratory burst oxidase homolog D (RbohD)-dependent mechanism in response to different stresses in Arabidopsis. *New Phytologist*, **213**, 1667–1681.

You, Y., **Huber, M.**, **Müller, R.D.**, **Poulsen, C.J.** & **Ribbe, J.** (2009) Simulation of the Middle Miocene Climate Cptimum. *Geophysical Research Letters*, **36**, L04702.

Zachos, J., **Pagani, M.**, **Sloan, L.**, **Thomas, E.** & **Billups, K.** (2001) Trends, rhythms, and aberrations in global climate 65 Ma to present. *Science*, **292**, 686–693.

Zachos, J.C., **Dickens, G.R.** & **Zeebe, R.E.** (2008) An early Cenozoic perspective on greenhouse warming and carbon-cycle dynamics. *Nature*, **451**, 279–283.

Zhang, H., **Fu, R.**, **Li, M.** ***et al.*** (2025) The key pathways in halophyte tree revealed via transcriptome analysis in response to salt stress. *Plant Growth Regulation*. Available from: https://doi.org/10.1007/s10725-025-01368-6

Zhou, X., **Li, J.**, **Wang, Y.**, **Liang, X.**, **Zhang, M.**, **Lu, M.** ***et al.*** (2022) The classical SOS pathway confers natural variation of salt tolerance in maize. *New Phytologist*, **236**, 479–494.

Zhu, R., **Shao, S.**, **Xie, W.**, **Guo, Z.**, **He, Z.**, **Li, Y.** ***et al.*** (2023) High-quality genome of a pioneer mangrove *Laguncularia racemosa* explains its advantages for intertidal zone reforestation. *Molecular Ecology Resources*, **25**, e13863.